AIP Advances

Alloy disorder modulated electron transport at $Mg_xZn_{1-x}O/ZnO$ heterointerface

Cite as: AIP Advances **7**, 015029 (2017); https://doi.org/10.1063/1.4974462
Submitted: 22 November 2016 . Accepted: 05 January 2017 . Published Online: 18 January 2017

Aswin Vishnuradhan, Y. Kozuka, M. Uchida, J. Falson, A. Tsukazaki, and M. Kawasaki

AIP ADVANCES **7**, 015029 (2017)

Alloy disorder modulated electron transport at $Mg_xZn_{1-x}O/ZnO$ heterointerface

Aswin Vishnuradhan,[1] Y. Kozuka,[1,a] M. Uchida,[1] J. Falson,[2] A. Tsukazaki,[3] and M. Kawasaki[1,4]

[1]*Department of Applied Physics and Quantum-Phase Electronics Center (QPEC), University of Tokyo, Tokyo 113-8656, Japan*
[2]*Max Planck Institute for Solid State Research, Heisenbergstrasse 1, D-70569 Stuttgart, Germany*
[3]*Institute for Materials Research, Tohoku University, Sendai 980-8577, Japan*
[4]*RIKEN Center for Emergent Matter Science (CEMS), Wako 351-0198, Japan*

(Received 22 November 2016; accepted 5 January 2017; published online 18 January 2017)

High-mobility electron systems in two dimensions have been the platform for realizing many fascinating quantum phenomena at low temperatures. Continuous demand to improve the sample quality has necessitated the investigations of various disorders influencing the quantum transport. Here, we study the effect of short-ranged alloy disorder on the scattering of two-dimensional electron system in $Mg_xZn_{1-x}O/ZnO$. For this purpose, we employ a modified interface profile consisting of $Mg_{0.01}Zn_{0.99}O/ZnO$ with a thin (2nm) $Mg_xZn_{1-x}O$ interlayer with x ranging from 0.005 to 0.4. This interlayer design allows us to investigate scattering mechanisms at a nearly constant carrier density as the interlayer is found not to significantly affect the carrier density but enhance alloy disorder. While the transport scattering time (τ_{tr}) shows a strong correlation with x, the quantum scattering time (τ_q) remains insensitive to x. The large variation in the τ_{tr}/τ_q ratio (from 16.2 to 1.5 corresponding to x from 0.005 to 0.4) implies a change in the dominant scattering mechanism from long range towards short range with increasing x. The insensitivity of τ_q on x indicates the scattering rate is not dominated by the alloy disorder. This implies that other scattering mechanisms, likely unintentional background impurities or remote surface disorders, are dominant in limiting τ_q, and therefore providing a prospect for pursuing ever higher levels in the quality of the two-dimensional electron system in $Mg_xZn_{1-x}O/ZnO$ system. [http://dx.doi.org/10.1063/1.4974462]

I. INTRODUCTION

High-mobility electrons in two dimensions have provided the foundation for a number of applications, such as high-frequency devices,[1] as well as to explore fascinating quantum phenomena.[2] While the discovery of new phenomena in these two-dimensional electron systems (2DES) always correlated with significant gains in the sample quality, new applications were also proposed over time which can employ high-quality heterostructures. For instance, the topological quantum computation[3] using even-denominator fractional quantum Hall states requires high-quality heterostructures for their successful realization, thus emphasizing the continuous demand to improve the sample quality.

The quality of 2DES is assessed by mobility (μ) as a measure of cleanness, which is related to transport scattering time (τ_{tr}) as $\mu = e\tau_{tr}/m^*$, where e is the elementary charge and m^* is the effective mass. Alternately, quantum scattering time (τ_q) is another measure of the cleanness directly reflecting the phase coherence of electrons. While all the scattering events are equally represented in

[a]Author to whom correspondence should be addressed. Electronic mail: kozuka@ap.t.u-tokyo.ac.jp

τ_q, backscattering events with a large scattering angle (θ) dominantly influence τ_{tr} over small-angle (forward) scattering events due to the $(1 - \cos\theta)$ weighting factor present in its definition.[4] Hence, in the absence of backscattering, very high values of τ_{tr} can be obtained even with high probability of forward scattering events. For example, in the case of remotely delta-doped high-mobility 2DES in AlGaAs/GaAs heterointerface, the reported maximum mobility exceeds 30 million $cm^2 V^{-1} s^{-1}$, which corresponds to $\tau_{tr} \sim 1$ ns.[5–7] However, the probability of small-angle scattering from the remote ionized dopants is not negligible, leading to about two orders of magnitude smaller value for τ_q ($\sim$ 10 ps). Therefore, the comparison between τ_{tr} and τ_q enables identification of the dominant scattering factors, giving invaluable knowledge for improving the quality of 2DES.[4,8,9]

In this context, it is interesting to investigate τ_{tr} and τ_q in the 2DES at the $Mg_xZn_{1-x}O$/ZnO heterointerface, which has recently attained a mobility exceeding 1 million $cm^2 V^{-1} s^{-1}$ (Refs. 9 and 10) and exhibited the unique fractional quantum Hall effect with even-denominator filling factors.[11,12] Unlike the 2DES in GaAs/AlGaAs, where a remote delta-doped layer is the source of the 2DES at the interface, the discontinuity of polarization on account of Mg doping between $Mg_xZn_{1-x}O$ and ZnO gives rise to accumulation of 2DES owing to the structural deformations of Zn and oxygen tetrahedra along c axis in the wurtzite crystal structure, which induces spontaneous polarization.[13,14] This polarization doping, being free from ionized dopants, is advantageous to achieving long scattering times. Without ionized dopants, the remaining possible sources of scattering would be unintentional background impurities, remote surface disorders, and alloy disorder[15,16] The influence of background impurities, causing long-range scattering potential, may be mitigated by increasing carrier density thereby enhancing screening or otherwise by drastic reduction of impurities themselves. On the other hand, the alloy disorder, acting as short-range scattering, is also associated with Mg content (x). Thus in the case of carrier accumulation by polarization discontinuity, the variation in x simultaneously changes the carrier density and scattering time/disorder, and hence influences of screening and alloy disorder cannot be independently studied.

In this study, in order to modulate the alloy disorder independently of carrier density, we have modified the interface of $Mg_{0.01}Zn_{0.99}O$/ZnO with inserting a thin ($\sim$ 2 nm) $Mg_xZn_{1-x}O$ interlayer where x ranges from 0.005 to 0.4. With this modification at the interface, we intend a systematic change in the short-range alloy disorder while limiting changes in charge density to be much lower than that associated with increasing the uniform doping of the capping layer. As a result, we find a significant decrease in τ_{tr} in the presence of the interface layer acting as a short-range scatterer, but a negligible change in τ_q. This indicates that alloy scattering is not a dominant factor even with large x in the $Mg_xZn_{1-x}O$ interlayer, and a fundamental decrease in the background impurities or remote surface disorders are necessary towards further advancement of quantum Hall physics.

II. EXPERIMENTAL

The films were grown by molecular beam epitaxy using pure ozone under identical growth conditions as reported previously.[10,17] The structure of the samples consisted of 500 nm-thick ZnO buffer layer followed by a 2 nm-thick $Mg_xZn_{1-x}O$ layer ($0.005 \leq x \leq 0.4$) and a 500 nm-thick $Mg_{0.01}Zn_{0.99}O$ capping layer as shown in the inset of Fig. 1(a). The typical growth rate was 600 nm/hour. For $x = 0.01$, this structure is the same as the standard sample with a single interface, which is denoted by "S" in Fig. 2. For magnetotransport measurements, indium contacts were soldered onto the edges of the 4×4 mm^2 samples cleaved out of the wafer in Van der Pauw geometry. The samples were measured with a ^{3}He cryostat for $T \geq 500$ mK and in a dilution refrigerator at further low temperatures.

III. RESULTS AND DISCUSSION

For obtaining an insight into the effects of the $Mg_xZn_{1-x}O$ interlayer, the potential profiles and electron distributions are calculated by solving the one-dimensional (1D) Schrödinger-Poisson equation using nextnano3 (Ref. 18) as shown in Fig. 1. Figure 1(a) shows the depth profiles of the conduction band edges for all the samples investigated in this study. The conduction band of the $Mg_{0.01}Zn_{0.99}O$ capping layer surface is assumed to be pinned at a potential of 0.9 eV, although the choice of this value does not make a significant difference in the following discussions. As shown

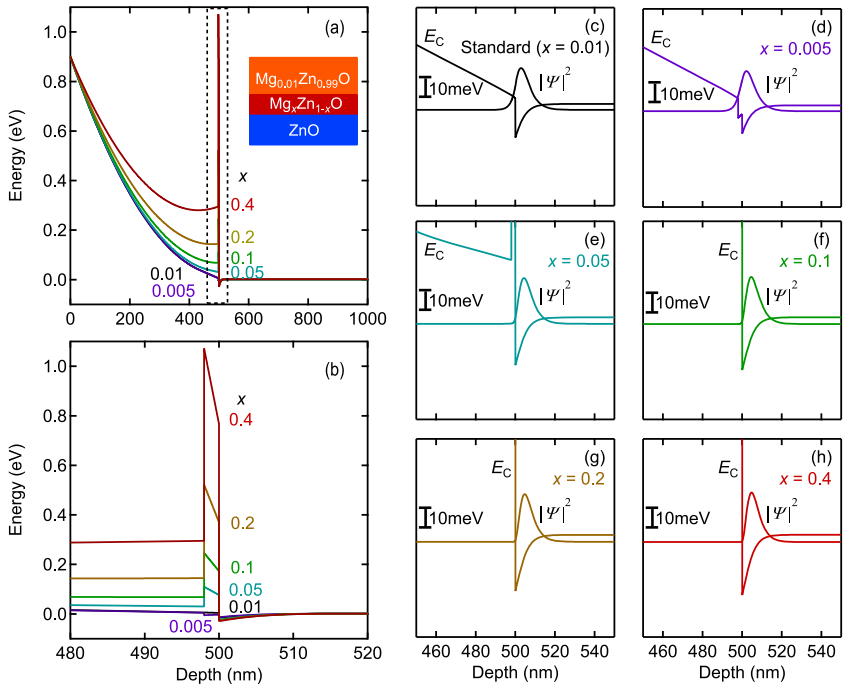

FIG. 1. (a) Calculated conduction band profiles of $Mg_{0.01}Zn_{0.99}O$(500nm)/ZnO heterostructures with thin (~ 2 nm) $Mg_xZn_{1-x}O$ interlayers and (b) their magnified views around the interfaces. (c)–(h) Calculated electron distribution $|\Psi|^2$ and conduction band profiles around the interfaces for each x ranging from 0.005 to 0.4. The inset in (a) is the schematic of the sample structure.

in Fig. 1(b) [magnification of Fig. 1(a) around the interfaces], the conduction band discontinuities between the ZnO and $Mg_xZn_{1-x}O$ layers increases as x increases. This modification in the potential profile leads to the variation of the electron distribution ($|\Psi|^2$) for different values of x as shown in Figs. 1(c)–1(h). As seen from the Figures, the electrons are more confined to the quasi-triangular quantum well with an increase in x. While a higher x could result in higher probability of alloy scattering, the electrons less distribute (penetrate) within the $Mg_xZn_{1-x}O$ layer due to the larger conduction band offset. The dominance of these competing effects is experimentally assessed by the mobility measurement as will be discussed subsequently.

Figure 2(a) shows the carrier density (n), extracted from the low-field Hall effect, for different x in the $Mg_xZn_{1-x}O$ interlayer. In order to compare the x dependence of carrier density for the samples investigated in the present study and that of the $Mg_xZn_{1-x}O$/ZnO samples with a single interface investigated in the previous study,[9] the carrier density at the lowest temperature is plotted as a function of x in Fig. 2(b). Compared to the previous experiments, the carrier density only modestly varies, thereby allowing us to selectively investigate effects of alloy disorder. The carrier density calculated by solving the 1D Schrödinger-Poisson equation also follows the same trend as the experimental value (solid black curve). For these samples, the mobility (μ) is plotted in Fig. 2(c) as a function of temperature. As in the previous study, the mobility shows a progressively upward increase down to 1 K, which is interpreted in terms of Bloch-Gruneisen regime for the acoustic phonons,[19,20] followed by saturating behavior below the temperature. The low-temperature mobility of the standard sample is comparable to that reported previously at the same x (Ref. 9). The low temperature mobility is plotted in Fig. 2(d) as a function of x in comparison with the mobility in the previous study with uniform Mg concentration in the barrier layer. μ decreases with increasing x, which indicates that the influence of alloy scattering in both sets of samples.

Here, it is noted that increasing Mg content in the $Mg_xZn_{1-x}O$ layer gives rise to two counter effects on electron mobility. With increasing Mg content, we expect that alloy scattering itself is enhanced, while the larger band discontinuity makes the fewer electrons distributed in the $Mg_xZn_{1-x}O$ layer, which may effectively reduce alloy scattering. In fact, we notice that the mobility of the sample

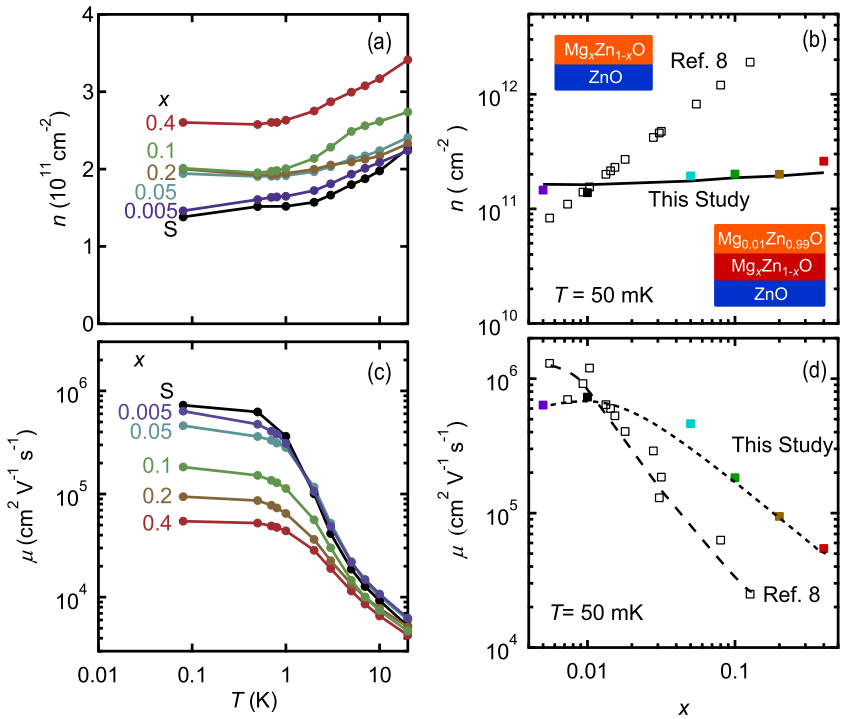

FIG. 2. Temperature dependence of (a) carrier density and (c) mobility for the $Mg_{0.01}Zn_{0.99}O$(500nm)/$Mg_xZn_{1-x}O$(2nm)/ZnO heterostructures. x dependence of (b) the carrier density and (d) mobility at T = 50 mK. In (b) and (d), the carrier density and the mobility are also plotted for $Mg_xZn_{1-x}O$(500nm)/ZnO heterostructures without the interlayer, which are taken from Ref. 8. The black curve in (b) is the total sheet carrier density calculated for Fig. 1. The dashed curves are guides to the eyes in (d). The insets in (b) are the schematics of the samples structures in this study and in Ref. 8.

with $x = 0.005$ is lower than the standard sample with $x = 0.01$ as a result of the enhanced penetration of electron distribution into the interlayer as shown in the calculations of Fig. 1(d). However, in the case of polarization doping, it is not generally easy to de-convolve the two contributions since the electron distribution and alloy disorder cannot be independently varied. On the other hand, in a standard semiconductor heterostructure such as in GaAs, the effect of alloy disorder has been selectively investigated using uniformly Al-doped $Al_xGa_{1-x}As$ quantum well structures with varying x.[21,22] In the ultra-high mobility 2DES of GaAs, alloy disorder was actually found to be a limiting factor of electron mobility,[21] and thus we may expect the same trend of mobility also in the case of ZnO 2DES.

In order to further investigate the scattering mechanism in detail, we examine small-angle scattering originating from the long-range potential, which is well evaluated by τ_q. To determine τ_q we describe the amplitude of the Shubnikov-de Hass (SdH) oscillations using the expression,[9,23] $\Delta R_{xx} = R_0 X(T) \exp\left(-\pi/\omega_c\tau_q\right)$, where $X(T) = \Psi/\sinh\Psi$ gives the thermal damping factor with $\Psi = 2\pi^2 k_B T/\hbar\omega_c$ and $\omega_c = eB/m*$. At a fixed temperature the plot of $\ln(\left(\Delta R_{xx}/4R_0 X(T)\right)$ vs $1/B$ (Dingle Plot) gives a straight line whose slope determines τ_q. Similarly, the effective mass can be evaluated from the temperature dependence of the SdH oscillations assuming τ_q to be temperature independent by plotting $\ln\left(\Delta R_{xx}/4R_0 T\right)$ vs T. An example of this procedure is depicted in Fig 3 for $x = 0.4$ sample. The temperature dependence of low field SdH oscillations is shown in Fig. 3(a). We adjusted the magnetic field angle (θ) against the 2DES plane so that the cyclotron energy and the Zeeman energy coincide [to the j ($= g^* m^*/2m_e\cos\theta$) = 2 coincidence condition, where g^* and m_e is the effective g-factor and the bare electron mass, respectively], the details of which are explained in Ref. 24. From this temperature dependence of the SdH oscillations we estimate the effective mass to be $m^* = (0.66 \pm 0.03)\ m_e$ (m_e is the bare electron mass) as shown in the inset of Fig. 3(a). With this value of the effective mass the quantum scattering time is estimated to be 14 ps from the slope of the

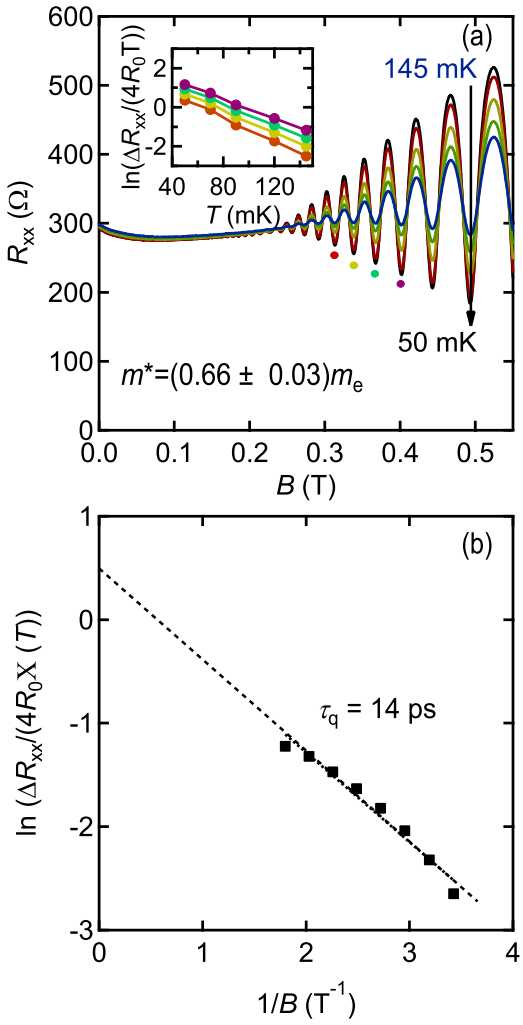

FIG. 3. (a) Temperature dependence of SdH oscillations from 50 mK to 145 mK for x = 0.4 sample. The inset shows the analysis to extract the effective mass (b) The dingle plot for x = 0.4 at 50 mK. The τ_q was determined to be 14 ps.

Dingle plot in Fig. 3(b). A slight non-linearity was seen in the dingle plots for all the samples at high magnetic fields indicative of small inhomogeneity in the samples,[23] which means the τ_q determined by this procedure would be slightly underestimated.[25] Similar analyses were made for all the samples for x = 0.005-0.4, resulting in similar effective masses of (0.7±0.1)m_e.

Given these analyses, x dependence of τ_{tr} and τ_q is plotted in Fig 4(a). In stark contrast to τ_{tr}, which decreases with increasing x, strikingly τ_q is nearly invariant even if Mg content x in the $Mg_xZn_{1-x}O$ interlayer varies by almost two orders of magnitude from 0.005 to 0.4. As τ_q equally takes into account all the scattering, including small-angle forward scattering and large-angle backward scattering, this result indicates that scattering probability is almost independent of x. The dominance of long-range potential over short-range potential can be parameterized by the ratio τ_{tr}/τ_q shown in Fig. 4(b). With increasing x, τ_{tr}/τ_q decreases from about 16 at x = 0.005 to 1.5 at x = 0.4, indicating that the scattering mechanism shows a crossover from long-ranged to short-ranged with increasing x. The value of $\tau_{tr}/\tau_q \sim 1$ at the highest x indicates almost isotropic scattering originating from dominant short-range alloy scattering. In contrast, for x = 0.005, τ_q is limited mainly by small-angle scattering likely from the background impurities or the remote surface disorders. The above behavior of τ_{tr} and τ_q are compared with a high-mobility 2DES in AlGaAs/GaAs. The ratio τ_{tr}/τ_q is about ~10 for background impurities and $\tau_{tr}/\tau_q > 10$ for remote surface charges.[26] Contrary to Ref. 9 (where the carrier density varies by an order of magnitude), at a nearly constant carrier density (corresponding to the highest mobilities) we

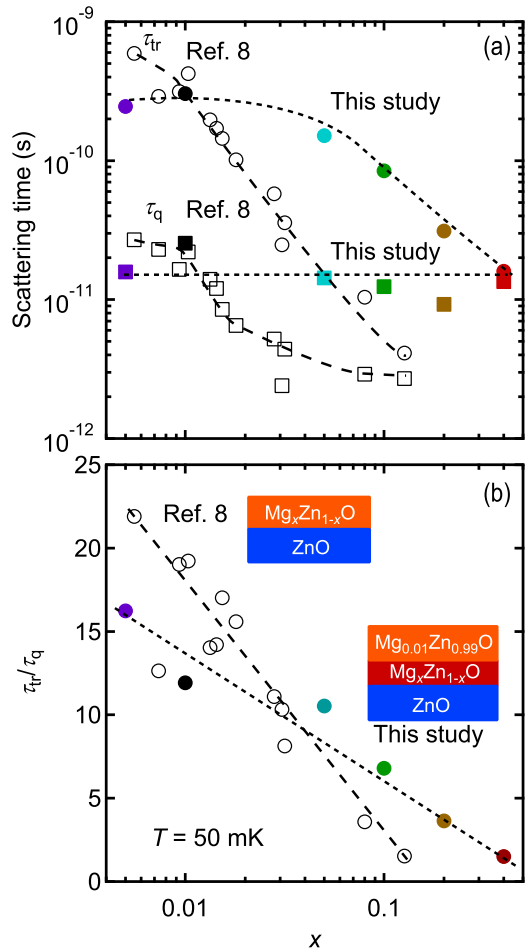

FIG. 4. x dependence of (a) scattering times (τ_{tr} and τ_q) and (b) the ratio τ_{tr}/τ_q for the $Mg_{0.01}Zn_{0.99}O$(500nm)/$Mg_xZn_{1-x}O$(2nm)/ZnO heterostructures. The same data are also plotted for $Mg_xZn_{1-x}O$(500nm)/ZnO heterostructures without the interlayer, which are taken from Ref. 8. The dashed curves are guides to the eyes. The insets in (b) are the schematics of the samples structures in this study and in Ref. 8.

find that the alloy disorder which apparently reduces μ (τ_{tr}) is not a dominant scattering mechanism in limiting τ_q. Theoretical studies on partially alloyed GaAs quantum wells have recently claimed the quantum scattering time to be limited only by remote ionized donors,[27] and experimentally the purity of Ga source was found to be a dominant factor.[7] As intentionally incorporated remote ionized donors are absent in ZnO heterostructures, the fundamental quality of 2DES in ZnO, measured by τ_q, can go far beyond that of GaAs by substantial reduction of background impurities.

IV. CONCLUSIONS

In summary, we have fabricated samples of $Mg_{0.01}Zn_{0.99}O/Mg_xZn_{1-x}O/ZnO$, where, alloy disorder is modulated preferentially over the charge density by modifying x. The analysis of the scattering times reveals that, with increasing x, the scattering is predominantly short-ranged, while long-range scattering is dominant at low x. The invariance of τ_q reveals that in the high mobility heterostructures, the quality as judged by the quantum scattering time is limited by factors other than alloy disorder hence giving insights for improving the quality in the future. Specifically, reducing the background impurity or remote surface disorders may be the most effective way to improve the fundamental quality of the 2DES in ZnO. Since the fascinating even-denominator fractional quantum Hall effect in GaAs has been found to relatively insensitive to alloy disorder, if this is also true for ZnO, we may

expect that the reduction of such extrinsic effects dramatically stabilize the recently found $\nu = 3/2$ quantum Hall state in ZnO,[11] which remains to be investigated in the future.

ACKNOWLEDGMENTS

We thank D. Maryenko for his helpful comments. This work was partly supported by Grant-in-Aids for Scientific Research (S) No. 24226002 from MEXT, Japan.

[1] T. Mimura, Jpn. J. Appl. Phys. **44**, 8263 (2005).
[2] K. von Klitzing, G. Dorda, and M. Pepper, Phys. Rev. Lett. **45**, 494 (1980).
[3] S. Das Sarma, M. Freedman, and C. Nayak, Phys. Rev. Lett. **94**, 166802 (2005).
[4] S. Das Sarma and F. Stern, Phys. Rev. B **32**, 8442 (1985).
[5] L.N. Pfeiffer and K.W. West, Physica E **20**, 57 (2003).
[6] V. Umansky, M. Heiblum, Y. Levinson, J. Smet, J. Nübler, and M. Dolev, J. Cryst. Growth **311**, 1658 (2009).
[7] G. C. Gardner, S. Fallahi, J. D. Watson, and M. J. Manfra, J. Cryst. Growth **441**, 71 (2016).
[8] S. Das Sarma and E. H. Hwang, Phys. Rev. B **90**, 035425 (2014).
[9] J. Falson, Y. Kozuka, J. H. Smet, T. Arima, A. Tsukazaki, and M. Kawasaki, Appl. Phys. Lett. **107**, 082102 (2015).
[10] J. Falson, Y. Kozuka, M. Uchida, J. H. Smet, T. Arima, A. Tsukazaki, and M. Kawasaki, Sci. Rep. **6**, 26598 (2016).
[11] J. Falson, D. Maryenko, B. Friess, D. Zhang, Y. Kozuka, A. Tsukazaki, J.H. Smet, and M. Kawasaki, Nat. Phys. **11**, 347 (2015).
[12] A. Tsukazaki, S. Akasaka, K. Nakahara, Y. Ohno, H. Ohno, D. Maryenko, A. Ohtomo, and M. Kawasaki, Nat. Mater. **9**, 889 (2010).
[13] A. Tsukazaki, A. Ohtomo, T. Kita, Y. Ohno, H. Ohno, and M. Kawasaki, Science **315**, 1388 (2007).
[14] Y. Kozuka, A. Tsukazaki, and M. Kawasaki, Appl. Phys. Rev. **1**, 011303 (2014).
[15] W. Walukiewicz, H. E. Ruda, J. Lagowski, and H. C. Gatos, Phys. Rev. B **30**, 4571 (1984).
[16] L. Hsu and W. Walukiewicz, Phys. Rev. B **56**, 1520 (1997).
[17] J. Falson, D. Maryenko, Y. Kozuka, A. Tsukazaki, and M. Kawasaki, Appl. Phys. Express **4**, 091101 (2011).
[18] S. Birner, T. Zibold, T. Andlauer, T. Kubis, M. Sabathil, A. Trellakis, and P. Vogl, IEEE Trans. Electron Devices **54**, 2137 (2007).
[19] D. Maryenko, J. Falson, Y. Kozuka, A. Tsukazaki, M. Onoda, H. Aoki, and M. Kawasaki, Phys. Rev. Lett. **108**, 186803 (2012).
[20] Q. Li, J. Zhang, J. Chong, and X. Hou, Appl. Phys. Express **6**, 121102 (2013).
[21] G. C. Gardner, J. D. Watson, S. Mondal, N. Deng, G. A. Csáthy, and M. J. Manfra, Appl. Phys. Lett. **102**, 252103 (2013).
[22] N. Deng, G. C. Gardner, S. Mondal, E. Kleinbaum, M. J. Manfra, and G. A. Csáthy, Phys. Rev. Lett. **112**, 116804 (2014).
[23] P. T. Coleridge, R. Stoner, and R. Fletcher, Phys. Rev. B **39**, 1120 (1989); P. Coleridge, Phys. Rev. B **44**, 3793 (1991).
[24] A. Tsukazaki, A. Ohtomo, M. Kawasaki, S. Akasaka, H. Yuji, K. Tamura, K. Nakahara, T. Tanabe, A. Kamisawa, T. Gokmen, J. Shabani, and M. Shayegan, Phys. Rev. B **78**, 233308 (2008).
[25] S. Syed, M. J. Manfra, Y. J. Wang, R. J. Molnar, and H. L. Stormer, Appl. Phys. Lett. **84**, 1507 (2004).
[26] S. J. MacLeod, K. Chan, T. P. Martin, A. R. Hamilton, A. See, A. P. Micolich, M. Aagesen, and P. E. Lindelof, Phys. Rev. B **80**, 035310 (2009).
[27] A. Rahmani, M. A. Sadeghzadeh, and R. Khordad, Superlattices Microstruct. **83**, 271 (2015).